Sinking krill carcasses as hotspots of microbial carbon and nitrogen cycling in the Arctic

Franco-Cisterna, Belén; Glud, Anni; Bristow, Laura A.; Rudra, Arka; Sanei, Hamed; Winding, Mie H.S.; Nielsen, Torkel G.; Glud, Ronnie N.; Stief, Peter

Published in:
Frontiers in Marine Science

Link to article, DOI:
10.3389/fmars.2022.1019727

Publication date:
2022

Document Version
Publisher's PDF, also known as Version of record

frontiers | Frontiers in Marine Science

TYPE Original Research
PUBLISHED 03 November 2022
DOI 10.3389/fmars.2022.1019727

OPEN ACCESS

EDITED BY
Travis Blake Meador,
Academy of Sciences of the Czech Republic (ASCR), Czechia

REVIEWED BY
Sairah Malkin,
University of Maryland, College Park, United States
Clara Manno,
British Antarctic Survey (BAS), United Kingdom

*CORRESPONDENCE
Belén Franco-Cisterna
belen@biology.sdu.dk

SPECIALTY SECTION
This article was submitted to Marine Biogeochemistry, a section of the journal Frontiers in Marine Science

RECEIVED 15 August 2022
ACCEPTED 20 October 2022
PUBLISHED 03 November 2022

CITATION
Franco-Cisterna B, Glud A, Bristow LA, Rudra A, Sanei H, Winding MHS, Nielsen TG, Glud RN and Stief P (2022) Sinking krill carcasses as hotspots of microbial carbon and nitrogen cycling in the Arctic.
Front. Mar. Sci. 9:1019727.
doi: 10.3389/fmars.2022.1019727

Sinking krill carcasses as hotspots of microbial carbon and nitrogen cycling in the Arctic

Belén Franco-Cisterna[1,2]*, Anni Glud[1,2], Laura A. Bristow[1], Arka Rudra[3], Hamed Sanei[3], Mie H.S. Winding[4], Torkel G. Nielsen[5], Ronnie N. Glud[1,2,6,7] and Peter Stief[1,2]

[1]Nordcee, Department of Biology, University of Southern Denmark, Odense, Denmark, [2]HADAL, Danish Center for Hadal Research, University of Southern Denmark, Odense, Denmark, [3]Lithospheric Organic Carbon (L.O.C.) Group, Department of Geoscience, Aarhus University, Aarhus, Denmark, [4]Greenland Climate Research Centre, Greenland Institute of Natural Resources, Nuuk, Greenland, [5]National Institute of Aquatic Resources, Technical University of Denmark, Kongens Lyngby, Denmark, [6]Department of Ocean and Environmental Sciences, Tokyo University of Marine Science and Technology, Tokyo, Japan, [7]Danish Institute for Advanced Study – DIAS, University of Southern Denmark, Odense, Denmark

Krill represent a major link between primary producers and higher trophic levels in polar marine food webs. Potential links to lower trophic levels, such as heterotrophic microorganisms, are less well documented. Here, we studied the kinetics of microbial degradation of sinking carcasses of two dominant krill species *Thysanoessa raschii* and *Meganyctiphanes norvegica* from Southwest Greenland. Degradation experiments under oxic conditions showed that 6.0-9.1% of carbon and 6.4-7.1% of nitrogen were lost from the carcasses after one week. Aerobic microbial respiration and the release of dissolved organic carbon were the main pathways of carbon loss from the carcasses. Ammonium release generally contributed the most to carcass nitrogen loss. Oxygen micro profiling revealed anoxic conditions inside krill carcasses/specimens, allowing anaerobic nitrogen cycling through denitrification and dissimilatory nitrate reduction to ammonium (DNRA). Denitrification rates were up to 5.3 and 127.7 nmol N carcass^{-1} d^{-1} for *T. raschii* and *M. norvegica*, respectively, making krill carcasses hotspots of nitrogen loss in the oxygenated water column of the fjord. Carcass-associated DNRA rates were up to 4-fold higher than denitrification rates, but the combined activity of these two anaerobic respiration processes did not contribute significantly to carbon loss from the carcasses. Living krill specimens did not harbor any significant denitrification and DNRA activity despite having an anoxic gut as revealed by micro profiling. The investigated krill carcasses sink

fast (1500-3000 m d^{-1}) and our data show that only a small fraction of the associated carbon is lost during descent. Based on data on krill distribution, our findings are used to discuss the potential importance of sinking krill carcasses for sustaining benthic food webs in the Arctic.

KEYWORDS

Biological carbon pump, marine snow, nitrogen, carbon, oxygen, krill, degradation, mineralization

Introduction

Euphausiids (krill) are a major component of marine food webs in polar ecosystems. They are consumers of pelagic primary producers and heterotrophic organisms (Agersted et al., 2014) and serve as prey for fish, seabirds, and marine mammals (Mauchline and Fisher, 1969). The ecological importance of krill as secondary producers is well documented, while their biogeochemical relevance has only recently gained recognition (Cavan et al., 2019; Manno et al., 2020; Pauli et al., 2021). Krill are presumed to be important contributors to the biological carbon pump in the ocean, transporting organic carbon and nutrients from the surface to deeper waters through diel vertical migration and the production of fast-sinking fecal pellets, exuviae, and carcasses (Berge et al., 2009; Cavan et al., 2019; Manno et al., 2020; Pauli et al., 2021). In the Southern Ocean, for example, krill-derived sinking particles represent >50% of the particulate organic carbon (POC) fluxes throughout the year, with particular relevance of fecal pellets in autumn, exuviae in summer, and carcasses in winter (Manno et al., 2020). The carbon flux through krill fecal pellets is attenuated by microbial degradation and fragmentation (Belcher et al., 2016; Pauli et al., 2021), while the microbial degradation of krill carcasses and exuviae during their descent remains unexplored. Those organic particles that escape degradation in the water column are deposited on the seabed where they represent a potentially important food source for benthic communities (Sokolova, 1994; Belcher et al., 2016; Manno et al., 2020) or are sequestered in the sediment.

The Arctic Ocean is an active site of biological production and carbon cycling (Wheeler et al., 1996; Chen et al., 2002). Near the surface, food webs are supported by sea ice algae and phytoplankton (Bourgeois et al., 2017), while the food supply of benthic heterotrophic communities is mostly limited to the vertical flux of particles from the euphotic zone (Werner, 2000; Gaillard et al., 2017). However, an imbalance between the carbon supply by primary production and the carbon demand of benthic organisms in the central Arctic Ocean has been documented (Wiedmann et al., 2020), suggesting the presence of unaccounted sources of organic matter in the passive carbon flux, such as zooplankton carcasses (Manno et al., 2020).

Carcasses are generally prevalent in zooplankton communities, accounting for 12–60% of the standing stock of marine zooplankton (Tang and Elliott, 2014). Copepod carcasses, for example, represent an important component of microbially-driven pelagic element cycling (Glud et al., 2015; Stief et al., 2017; Tang et al., 2019). Fresh copepod carcasses provide dissolved organic carbon to free-living pelagic microbes, while older carcasses may supply particulate organic carbon to the ocean interior, especially in low-temperature regions where carcass mineralization rates are low (Franco-Cisterna et al., 2021; Halfter et al., 2022). Copepod carcasses contribute also to microbial nitrogen cycling (N-cycling) in the pelagic zone. Large copepod species may harbor an oxygen-depleted interior (Tang et al., 2011; Glud et al., 2015) where different pathways of anaerobic N-cycling can take place, even in the otherwise oxic water column (Glud et al., 2015; Stief et al., 2017; Stief et al., 2018). Denitrification, dissimilatory nitrate reduction to ammonium (DNRA), and anaerobic ammonium oxidation (anammox) have been detected in live copepods and carcasses of copepods and ostracods (Stief et al., 2018; Glud et al., 2015; Stief et al., 2017). Canonical denitrification and DNRA are coupled with the oxidation of organic matter and may thus contribute to carcass-carbon mineralization. Denitrification and anammox release N_2 and N_2O into the ambient water and thereby enhance the pelagic nitrogen loss (N-loss) from the oceans (Thamdrup, 2012). Due to their large body size, krill may also provide anoxic microenvironments that support anaerobic N-cycling, but its occurrence and potential importance for polar marine ecosystems remain unexplored.

In Arctic waters, the Arctic krill *Thysanoessa raschii* and the northern krill *Meganyctiphanes norvegica* occur in high abundance along the coast of Norway, Iceland, Greenland, Alaska, the Bering Sea, the East Siberian Sea, and the Barents Sea (Falk-Petersen et al., 1981; Berline et al., 2008; Agersted and Nielsen, 2014; McBride et al., 2014; Silva et al., 2017; Ershova and Kosobokova, 2019). In fjords, they overlap spatially and temporally, but differences in behavior, life cycle strategies, and predation over a wide prey-size spectrum allow them to coexist (Agersted et al., 2014). The different species traits may influence the microbial communities associated

with live krill and, consequently, the microbial processes driving the microbial degradation of the specimens upon death. Natural mortality for adult populations of *T. raschii* and *M. norvegica* account for 0.15% d^{-1} (Lindley, 1980) and 0.22% d^{-1} (Tarling, 2010), respectively, with predation exerting the strongest control. However, other causes like parasitic infections (Gómez-Gutiérrez et al., 2003) and infrequent freshwater intrusion from melting glacial ice (Fuentes et al., 2016) may result in a massive die-off of hundreds to thousands of carcasses m^{-2}, in which the element cycling is still undetermined.

The current study explored the microbial carbon and nitrogen cycling associated with degrading carcasses of *T. raschii* and *M. norvegica* that were experimentally produced and incubated in the laboratory. Carbon cycling was studied by following carcass-associated microbial respiration and the release of dissolved organic matter under oxic conditions for one week of simulated sinking. The reactivity of different organic carbon fractions in the carcasses in different degradation stages was characterized by pyrolytic analysis. Since O_2 micro profiling inside krill carcasses and guts of live krill revealed anoxic conditions, anaerobic N-cycling associated with krill carcasses and live krill was quantified by ^{15}N tracer experiments. The results were used to evaluate the quantitative contribution of krill carcasses to both carbon export and pelagic N-loss in polar marine ecosystems.

Material and methods

Study site and krill sampling

Sampling was conducted in May 2019 in the area of Nuup Kangerlua, Southwest Greenland (64.8°N 51.8°W) (Figure 1A). Nuup Kangerlua is a sub-arctic fjord with a maximum depth of 625 m. It is characterized by a temperature and salinity gradient from the warm (2.0–3.5°C) and salty (32.8–33.5) water at the mouth of the fjord to the colder (-0.6–4.8°C) and fresher (21.5–33.5) water in the innermost part (Mortensen et al., 2011; Agersted and Nielsen, 2016). In the fjord, the krill species *Thysanoessa raschii, T. inermis, T. longicaudata*, and *Meganyctiphanes norvegica* are differently distributed according to the hydrography (Agersted and Nielsen, 2016). The targeted species in this study were the omnivorous-herbivorous *T. raschii* (Figure 1B), of approx. 20 mm in length and abundant at the mouth and the main basin of the fjord, and the omnivorous-carnivorous *M. norvegica* (Figure 1C) of approx. 40 mm in length that dominates the inner part of the fjord (Agersted et al., 2014).

Specimens of *T. raschii* and *M. norvegica* were collected at two stations (Figure 1) on board the R/V SANNA (Greenland Institute of Natural Resources). Samples were taken at night from 160 m depth using a mid-water ring net (MIK, 1500 µm mesh size) with oblique tows. On board, the cod end was immediately transferred to a large container with seawater (100 L), and the samples were fed with a monoculture of the diatom *Thalassiosira weissflogii*. The samples were returned to the Greenland Institute of Natural Resources in Nuuk within 12 h and kept alive in a cold room at 2°C, a suitable temperature for both species (McQuinn et al., 2015), for 15 days. The two krill species were fed with *T. weissflogii* and natural zooplankton samples. Carcasses and animals in poor condition characterized by slow and erratic movements were removed from the container every day. Carcasses were removed at a rate of 2.8 and 2.6% d^{-1} for *T. raschii* and *M. norvegica*, respectively. In total, ca. 60 specimens of *T. raschii* and ca. 40 specimens of *M. norvegica* in the adult stage were used for the different experiments and analyses.

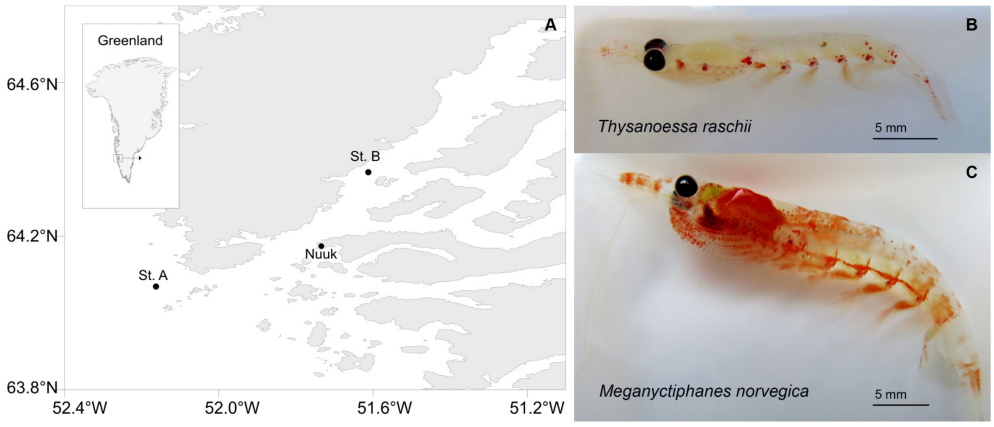

FIGURE 1
Study site and krill species. **(A)** Nuup Kangerlua fjord in Southwest Greenland. Black circles indicate the 2 sampling stations where krill was collected. **(B)** *Thysanoessa raschii* collected at the station (St.) A. **(C)** *Meganyctiphanes norvegica* collected at St. B.

Experimental procedure

Carcasses of *T. raschii* and *M. norvegica* were produced by suffocating krill specimens by anoxia exposure (<10 µmol O_2 L^{-1}) for 2 hours (Franco-Cisterna et al., 2021). The death of the animals was confirmed by the lack of movement after poking with a needle and the passive sinking even after exposure to fully oxygenated seawater.

Freshly produced carcasses were incubated in bottles filled with oxygenated seawater to study microbial carbon- and nitrogen cycling (Supplementary Figure S1). One carcass each was transferred to acid-washed glass bottles of different volumes according to krill size (26 mL and 120 mL for *T. raschii* and *M. norvegica*, respectively) and filled with 3-µm-filtered seawater from the sampling site. To allow the simultaneous analysis of aerobic and anaerobic microbial pathways, the seawater was air-saturated by flushing with a mixture of 20% O_2 and 80% He (thereby keeping the background concentration of N_2 low) and amended with $^{15}NO_3^-$ at a final concentration of ~10 µM, equivalent to 2.5-fold the ambient NO_3^- concentration. The bottles were sealed with deoxygenated (> 2 months in He atmosphere) butyl stoppers to enable sample extraction with syringes. For *T. raschii* and *M. norvegica*, 6 and 7 replicate bottles, respectively, were incubated; as controls without carcasses, 6 replicate bottles were filled with 3-µm-filtered, 20% O_2 and 80% He-flushed and $^{15}NO_3^-$ amended seawater. All bottles were mounted on a plankton wheel rotating at 15 rounds per minute to keep the carcasses suspended in the seawater. The experiments were run in darkness and at 2°C for one week.

Samples were collected at 7-15 different time points during the incubation using two syringes inserted simultaneously through the butyl stopper. The first syringe was filled with 4 mL (*T. raschii* incubations) or 10 mL (*M. norvegica* incubations) of new seawater prepared in the same way as for the initial filling (i.e., 3-µm-filtered, He-flushed and $^{15}NO_3^-$ amended seawater), while the second syringe was intended for sample extraction. The injection of new seawater from the first syringe automatically filled the second syringe with seawater from the incubation bottle. This reciprocal use of the two syringes was repeated twice to allow good mixing of the new seawater and the sample seawater. The collected sample was divided into subsamples for analysis of labeled N compounds, dissolved inorganic nitrogen (DIN), dissolved organic nitrogen (DON), dissolved organic carbon (DOC), and microbial abundance (Supplementary Figure S1. See details below).

Oxygen consumption in carcass incubations

Oxygen concentration in all incubation bottles was followed over time using oxygen-sensitive optodes mounted on the inner bottle wall that were interrogated from the outside by a FireSting Oxygen Meter (PyroScience, Aachen, Germany) every 3 hours, on average. A one-point calibration at 100% air saturation was made in the bottles with optode sensors before the experiments. The signals of the optode sensors at 0% air saturation were checked in dithionite amended, i.e., anoxic seawater, at the end of the incubations and were always very close to the expected reading of zero. The generally observed decrease in oxygen concentration over time was ascribed to aerobic microbial respiration. Oxygen consumption due to other processes (i.e., oxidation of sulfur compounds) was assumed to be minor. Microbial respiration rates were calculated from the decrease in oxygen concentration in the incubation bottles over time. The obtained 'total respiration rate' corresponds to the sum of microbial respiration activity associated directly with the carcass and microbial respiration activity in the surrounding seawater.

To quantify microbial respiration activity directly associated with the carcass, two different methods were used. First, carcass-associated microbial respiration was taken as the difference between the total respiration rate in the incubation bottle and the respiration rate measured in the surrounding seawater alone after being in contact with the carcasses and therefore accounting for the potential impact of nutrients and/or microbes released from the carcasses. To assess this, the *T. raschii* carcasses were removed at selected time points and transferred to new seawater-filled bottles in which the overall incubation was continued. The seawater remaining in the old bottle was re-oxygenated. In *M. norvegica* incubations, 26 mL of seawater was transferred into a new bottle and re-oxygenated. The old bottle containing the *M. norvegica* carcass was filled up with new seawater to continue the overall incubation. The respiration measurements in the seawater previously exposed to the carcasses of both krill species continued for 4-8 time points at a time interval between 3 to 17 hours. Second, carcass-associated microbial respiration was measured in a flow-through system (Supplementary Figure S2). With this method, 3-µm-filtered seawater passed the carcass relatively fast (at a flow rate of 0.7 mL min^{-1}) and only once, thereby ruling out contributions from respiration activity by growing bacterial populations in the seawater. For this measurement, one carcass at a time was inserted into a glass tube of 10 mm inner diameter and 58 mm length. At both ends of the glass tube, a plastic T-shaped tube was connected. Through each of the T-tubes, one custom-made oxygen-sensitive optode with a tip diameter of 40 µm was placed vertically into the stream of seawater passing by the carcass. A nylon net (1 mm pore size) was placed between the glass tube and the T-tubes to prevent the carcass from drifting out of the tube. The flow-through system was placed in a thermoregulated water bath at 6.0°C, the lowest temperature that could be achieved in the laboratory. Oxygen concentration in the flowing seawater was measured with a FireSting Oxygen Meter (PyroScience, Aachen, Germany) before and after passing by the carcass. The carcass-associated microbial respiration rates were calculated as the difference in the oxygen concentration between the two optodes multiplied by the flow rate. Using the flow-through system, microbial respiration was measured in 1 carcass

of *T. raschii* and 4 carcasses of *M. norvegica* in independent measurements. Carcass-associated respiration rates were divided by the total carbon content of the carcasses to calculate carbon-specific respiration rates, according to Iversen and Ploug (2013).

Oxygen concentration inside krill guts

To determine if krill have an oxygen-depleted interior, oxygen micro profiles in the gut of live and dead krill were measured in 5-6 specimens per species. Oxygen concentration was firstly measured in live organisms because anaerobic processes were studied in both live and freshly killed krill. Fed and starved krill were compared because food can affect the oxygen levels inside zooplankton guts (Tang et al., 2011). For this, a two-strand braided metal wire (500 µm diameter) was attached to the cephalothorax of each animal with a small drop of superglue (Superlim 1, Bostik). The other end of the wire was fastened to the wax bed in a petri dish. This arrangement was placed in a thermoregulated water bath at 6.7 ± 1.1°C with filtered and air-saturated seawater. Using a stereomicroscope and a micromanipulator, the tip of a calibrated 'Clarke-type' O_2 microelectrode (Revsbech, 1989) with a tip diameter <10 µm was moved from the area enclosed by the telson and uropods towards the anus of the immobilized animal (Figure 2). The sensor was moved in steps of 50 µm towards and into the animal and 3 to 5 oxygen micro profiles were measured per individual.

Anaerobic nitrogen cycling

Since oxygen micro-profiling indicated anoxic conditions in the gut of live and dead krill, the occurrence of active anaerobic N-cycling in both live krill and carcasses was tested. To study anaerobic N-cycling on live krill, the experimental settings described above for carcasses (see section Experimental procedure) were applied with some modifications. First, incubations were performed for 24 h. Second, 5 replicates with one animal each and 5 controls with seawater only were incubated. Third, anaerobic N-cycling was tested in starved and fed animals of both species.

The rates of denitrification and DNRA production in both live krill and carcass incubations were measured using a ^{15}N isotope labeling approach under oxic conditions. At different time points, 1.5 or 3 mL of seawater was sampled and transferred into a helium-flushed and half-evacuated exetainer (Labco, U.K.) containing 50 µL of $ZnCl_2$ and stored upside-down at ambient temperature until analysis (Stief et al., 2016). ^{15}N-N_2 was analyzed in the headspace of the exetainer samples on a gas chromatography-isotopic ratio mass spectrometer (GC-IRMS, Delta V Plus, Thermo Scientific) as described in Dalsgaard et al. (2012). After sampling the headspace of the exetainers for ^{15}N-N_2, an aliquot of the liquid sample was used to measure $^{15}NH_4^+$ production rates. To this end, $^{15}NH_4^+$ was chemically converted to ^{15}N-N_2 through the hypobromite assay (Warembourg, 1993), followed by a ^{15}N-N_2 analysis on the GC-IRMS. Denitrification and DNRA rates were calculated from the change in $^{30}N_2$ and $^{15}NH_4^+$ concentrations over time, respectively, the labeling fraction of NO_3^-, and the successive dilution due to repeated sampling (Stief et al., 2016). The minimum, maximum, and mean denitrification and DNRA rates were standardized to carcass biomass by dividing the respective rate by the total carbon content per carcass. All rates presented here were measured at oxygen concentrations >100 µM O_2 in the incubation bottles (Supplementary Figure S3).

Release of dissolved compounds

The release of dissolved organic carbon (DOC), dissolved organic nitrogen (DON), and dissolved inorganic nitrogen (DIN) due to carcass degradation was measured in seawater samples collected at different time points and stored at -80 °C. DOC and DON concentrations were measured in 1-mL samples on a TOC analyzer (TOC-L Shimadzu). DIN concentrations were measured in 0.3-mL samples using a spectrophotometric assay for NH_4^+ (Bower and Holm-Hansen, 1980). Rates of DOC, DON, and NH_4^+ release were calculated from the increase in concentrations over time and corrected for successive dilution due to repeated sampling.

Bacterial production

Bacterial abundance was measured in seawater samples collected from the incubation bottles at different time points. After sampling, 1 mL of seawater was preserved with 50 µL formaldehyde 37% (~2% final concentration), kept at 4°C overnight, and then stored at -20°C. For the analysis, the samples were completely thawed, stained with SYBR Green I, and measured on a flow cytometer (BD FACSAria II cell sorter – BD Biosciences). Carbon assimilated into biomass (bacterial production, BP) was calculated assuming a bacterial growth efficiency (BGE) of 0.15 (Kirchman et al., 2009), and the total aerobic bacterial respiration (BR) measured in this study, according to the equation, $BP = \frac{(BGE \star BR)}{(1-BGE)}$ (Del Giorgio and Cole, 1998). Microbial nitrogen assimilation for biomass production was estimated from a general C:N ratio of 6.8 for marine bacterial cells (Fukuda et al., 1998).

Carbon and nitrogen loss from sinking krill carcasses

To determine the total loss of carbon from the carcasses, four different pathways were considered: Particulate organic carbon (POC) oxidation through aerobic microbial respiration, POC oxidation through anaerobic N-cycling pathways (i.e.,

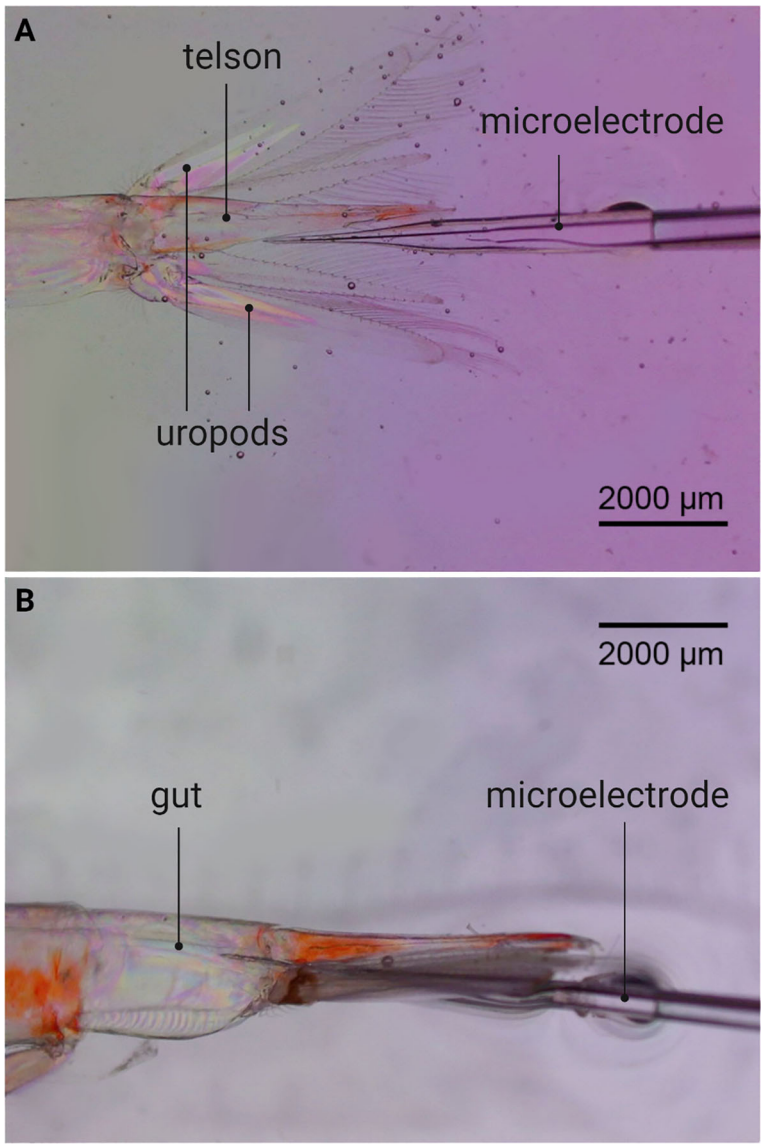

FIGURE 2
Oxygen micro-profiling of krill guts. **(A)** Microelectrode in the area enclosed by the telson and uropods of *Meganyctiphanes norvegica*, before entering the krill gut. **(B)** Microelectrode inside the gut of *M. norvegica*.

denitrification and DNRA), DOC release from the carcasses, and bacterial production. To calculate carbon mineralization rates due to aerobic microbial respiration, oxygen consumption rates were converted to carbon oxidation rates assuming a respiratory quotient (RQ) of 0.8. The same procedure was applied to quantify the carbon oxidized through anaerobic N-cycling pathways with RQs of 1.25 and 2.0 for denitrification and DNRA, respectively. Particulate organic nitrogen (PON) mineralization producing ammonium, DON release from the carcasses, and bacterial production were considered to determine the total loss of organic nitrogen from the carcasses.

The total carbon and nitrogen loss from krill carcasses were calculated as the sum of the rates of the processes listed above. Cumulative carbon and nitrogen loss from the carcasses were expressed relative to the total organic carbon and nitrogen content of fresh carcasses, quantified on an elemental analyzer coupled to an isotope ratio mass spectrometer (Delta V Advantage IRMS with Thermo Scientific EA) in 5 carcasses of *T. raschii* and 2 carcasses of *M. norvegica*.

Particulate organic carbon fractions

Different POC fractions in the krill tissues were quantified by pyrolysis in *T. raschii* and *M. norvegica* carcasses of different ages, ranging from 0.5 to 7 days of degradation. For the analysis, the samples were freeze-dried and finely ground. Approximately 2 mg of carcass sample mixed with 50 mg of sand were analyzed by the programmed-temperature method HAWK® anhydrous pyrolysis (Wildcat Technologies, USA) and Total Organic Carbon (TOC) Instrument (Rudra et al., 2021). To accurately quantify the pyrolysable organic carbon fractions, the pyrolysis-TOC analysis was coupled with continuous extended slow heating (ESH®; PetroEval ApS, Denmark) pyrolysis analysis (Sanei et al., 2015). For pyrolysis-TOC analysis, the samples were pyrolyzed at 300°C for 5 minutes and then ramped at 25°C min^{-1} up to 650°C, followed by the oxidation cycle beginning at 300°C and a heating ramp of 25° C min^{-1} up to 850°C. The TOC was determined as a sum of pyrolysable organic carbon (OC) evolved during pyrolysis and the residual OC evolved during the oxidation stage (Lafargue et al., 1998). The ESH pyrolysis cycle starts at 100°C (3 minutes hold) followed by a temperature ramp of 10°C min^{-1} up to 650°C.

Hydrocarbons (HC) released during pyrolysis were measured as different peaks and classified according to their lability/degradability. Lability is a continuum of the decomposition turnover times resulting from the interaction between the chemical composition of the organic matter and the microbial metabolic capacity (Ostapenia et al., 2009; Nelson and Wear, 2014). However, a pragmatic approach for expressing the different organic fractions in this study was the categorization as labile, semi-labile, and semi-refractory. The labile fraction represents the HC released from 100°C to 200°C during ESH, the semi-labile fraction represents the HC released from 225°C to 400°C during ESH, and the semi-refractory fraction represents the sum of HC peaks evolved from ESH 400°C to 650°C, the residual OC fraction and the oxygen-containing OM fractions released during pyrolysis. Both labile and semi-labile fractions are readily degradable, while semi-refractory fraction represents bio-macromolecular structures of the organisms with high preservation potential (Sanei et al., 2015). Each fraction was normalized to the TOC measured by the HAWK. The relative changes in the percentages of organic carbon fractions were followed over time and converted to absolute units according to the calculated amount of carbon lost per day.

In vitro carcass sinking rates

Carcasses of similar sizes from the two species were used to measure the sinking rates in the laboratory. *T. raschii* carcasses ranged between 2.3 and 2.5 cm and *M. norvegica* carcasses ranged between 4.1 and 4.6 cm. Individually, 5 carcasses per species were placed at the center of the water surface in a graduated cylinder filled with 500 mL seawater equilibrated to the ambient temperature in a cold room (2°C). The sinking rates were measured as the time it took for the carcass to descend 18 cm. The rates were extrapolated to m d^{-1}.

Statistical analyses

The temporal decrease in the different organic fractions was checked for significance using a one-sample t-test on the slope of the corresponding regression line. The same analysis was used to test if rates of denitrification and DNRA were significantly different from 0 on live krill and to assess differences in total carbon and nitrogen mineralization between the two krill species. This analysis was applied after testing that samples came from normally distributed populations with equal variances. In cases where data were not normally distributed, non-parametric tests were used. To identify differences in the overall average of aerobic microbial respiration, the release of dissolved compounds, and rates of anaerobic N-cycling between the two krill species, a non-parametric Mann-Whitney rank-sum test was used. The same statistical analysis was used to assess differences in the overall average of denitrification vs DNRA rates, and NH_4^+ vs DON release within each krill species. To identify differences in the contribution of aerobic and anaerobic processes, and bacterial production to carbon loss, a non-parametric Kruskal-Wallis one-way ANOVA on ranks analysis was used followed by the Tukey *post-hoc* test. All tests were performed at a significance level of $\alpha = 0.05$ in the statistical software SigmaPlot Version 11.0.

Results

Aerobic microbial respiration

Total respiration rates associated with carcasses of both krill species increased over time (Figures 3A, B) and were significantly higher in *M. norvegica* than in *T. raschii* carcasses (Mann-Whitney, $U = 0$, $p < 0.001$, $n1 = 8$, $n2 = 9$). Maximum respiration activity was measured after 7 days of degradation with rates of 15.2 ± 2.6 µmol O_2 $carcass^{-1}$ d^{-1} and 48.9 ± 9.5 µmol O_2 $carcass^{-1}$ d^{-1} for *T. raschii* and *M. norvegica*, respectively (mean ± standard deviation, n = 6-7). However, the difference was related to the size difference of carcasses and on average, the carbon-specific respiration rates calculated for *T. raschii* and *M. norvegica* carcasses were similar (Supplementary Table S1). For both krill species, respiration activity in the seawater reached a maximum on day 4 of the incubation and then decreased again (Figures 3A, B), while carcass-associated microbial respiration activity showed the opposite trend (Figures 3C, D). The carcass-associated microbial respiration measured in the flow-through system was generally in the same range or only slightly higher than the rates calculated for the bottle incubations (Figures 3C, D). Calculating the mean respiration activity in the bottles during the entire incubation period indicates that 50 ± 26% and 57 ± 25% of the oxygen consumption was directly associated

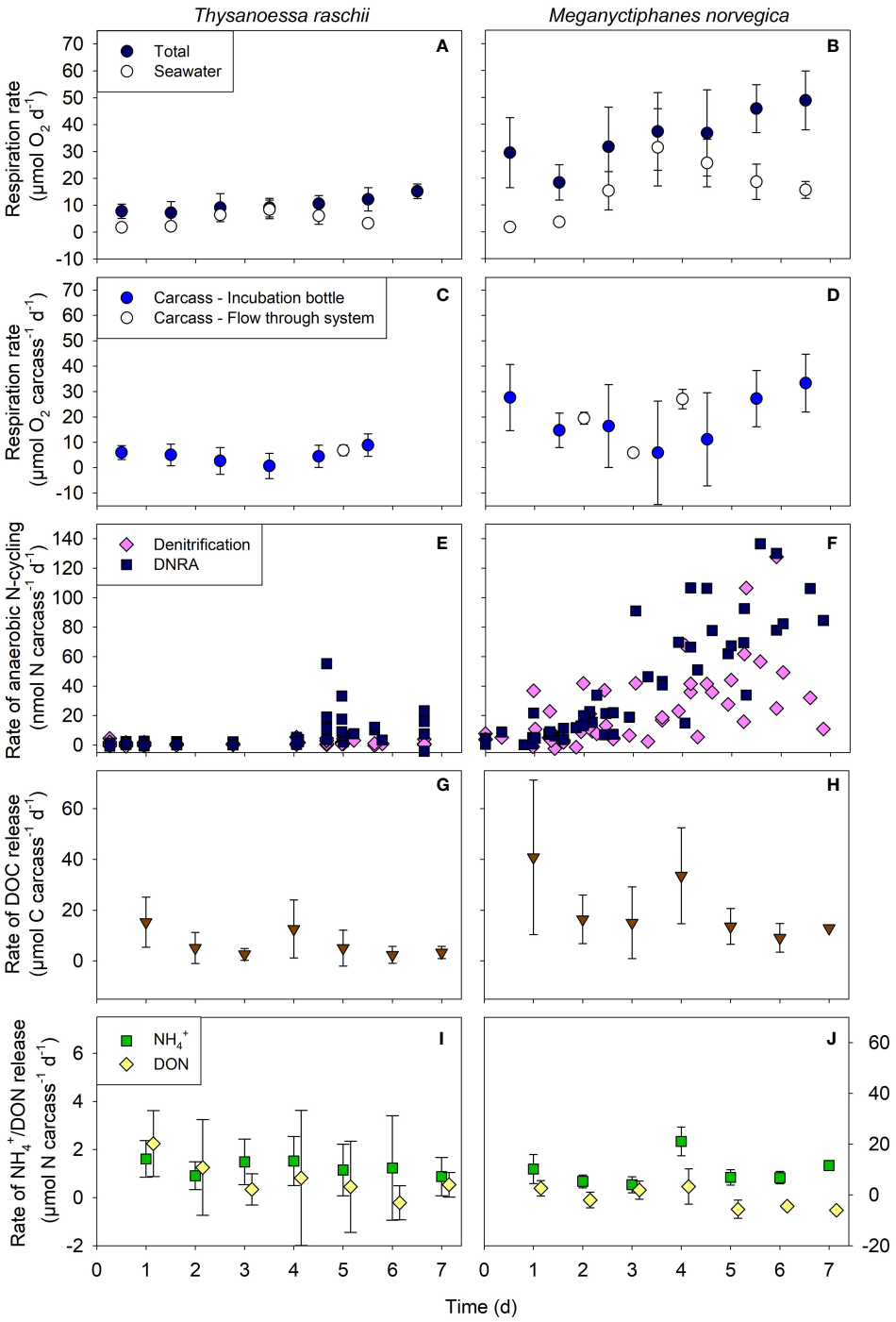

FIGURE 3
Rates of different aerobic and anaerobic processes measured in carcasses of *Thysanoessa raschii* (left panels) and *Meganyctiphanes norvegica* (right panels). **(A, B)** Total and seawater-associated microbial respiration rates. **(C, D)** Calculated carcass-associated microbial respiration in incubation bottles and the flow-through system. **(E, F)** Rates of denitrification and dissimilatory nitrate reduction to ammonium (DNRA). **(G, H)** Rates of Dissolved Organic Carbon (DOC) release. **(I, J)** Rates of ammonium (NH_4^+) and Dissolved Organic Nitrogen (DON) release. Mean and standard deviations of 6-7 replicates are shown.

with carcasses of *T. raschii* and *M. norvegica*, respectively, and the remainder was respired by microbes in the ambient water.

Oxygen concentration inside krill guts

Oxygen micro profiling revealed anoxic guts in both krill species irrespective of the feeding status of the animal. Oxygen concentration decreased from 313 µM in the surrounding seawater to 0 µM when the microelectrode entered the gut (Figure 4). A decrease in oxygen concentration was already observed in the area enclosed by the telson and uropods of the animals (Figure 2A). One micro-profile (Figure 4B) was measured in a dead animal, confirming that the anoxic conditions of live krill guts persist in the carcasses.

Anaerobic N-cycling

Two pathways of anaerobic N-cycling were detected in the oxygen-depleted carcasses of both krill species: denitrification and DNRA (Figures 3E, F). There were no indications of significant anammox activity since $^{29}N_2$ production rates were not higher than expected from random isotope pairing during denitrification. In *T. raschii* carcasses, denitrification rates were constantly low, while DNRA rates were initially low and then increased after 4 days of degradation (Figure 3E). In *M. norvegica* carcasses, the rates of both processes increased gradually over time after only a one-day lag phase (Figure 3F) and were significantly higher than in *T. raschii* carcasses (Mann-Whitney, U = 573 (denitrification), U = 876 (DNRA), $p < 0.001$, n1 = 59, n2 = 62). DNRA rates increased more strongly than denitrification rates in *M. norvegica* carcasses, but the overall average rates of both pathways were not significantly different (Mann-Whitney, U = 1455, p = 0.125, n1 = n2 = 59).

In live specimens of both krill species, there were no indications of denitrification and DNRA irrespective of the feeding status of the animals (Table 1) since the rates were generally not significantly different from zero (Supplementary Table S2).

Release of dissolved compounds and bacterial abundance

Rates of DOC release tended to be higher at the beginning than at the end of the carcass incubations for both krill species, but the scatter of data at each time point was high (Figures 3G, H). On day 4, relatively high rates of DOC release were noted for

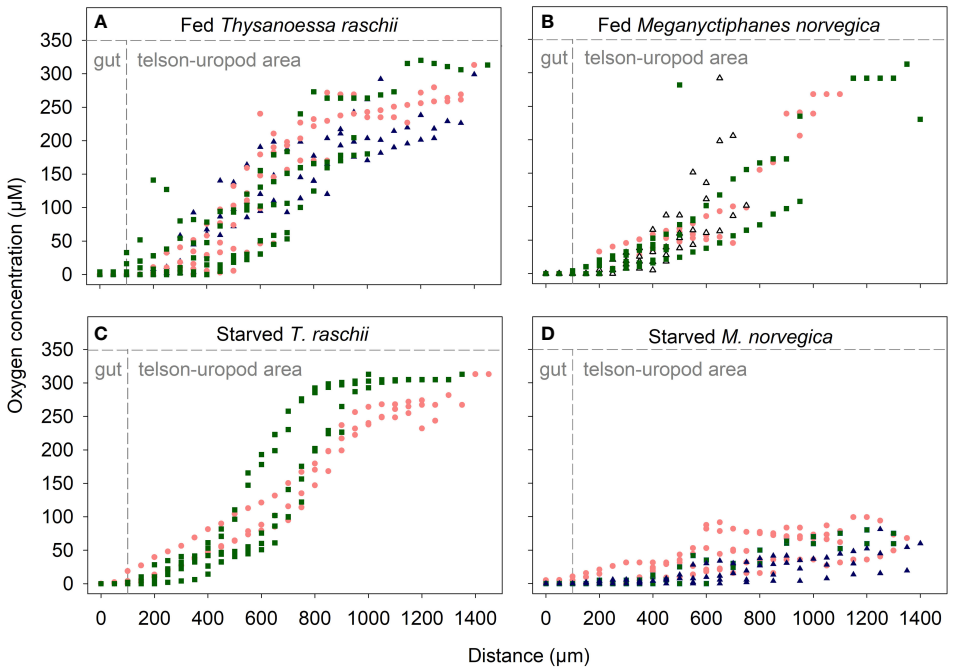

FIGURE 4
Oxygen micro profiles towards the guts of krill specimens with different feeding statuses. **(A)** Fed *Thysanoessa raschii*. **(B)** Fed *Meganyctiphanes norvegica*. **(C)** Starved *T. raschii*. **(D)** Starved *M. norvegica*. Each color/shape of the symbols corresponds to several micro profiles on the same individual. Triangles in panel B depict the micro profiles of one dead specimen. Panel sectors bordered by dashed lines depict different microenvironments where oxygen concentration was measured. Microsensors were moved from the area enclosed by the telson and uropods of krill towards the guts.

TABLE 1 Mean ± SD rates of denitrification and dissimilatory nitrate reduction to ammonium (DNRA) production in live krill (fed and starved) (n= 5), and carcasses (n= 6-7) of *Thysanoessa raschii* and *Meganyctiphanes norvegica*.

Species	Incubation	Denitrification rate (nmol N d^{-1})	DNRA rate (nmol N d^{-1})
T. raschii	Fed krill	0.3 ± 2.7	1.0 ± 2.8
	Control	0.4 ± 3.2	1.9 ± 3.0
	Starved krill	0.0 ± 1.5	1.5 ± 4.4
	Control	-0.6 ± 2.3	0.6 ± 0.8
	Carcass	1.0 ± 3.2 *	8.3 ± 30.7 *
	Control	-0.1 ± 0.1	0.0 ± 0.1
M. norvegica	Fed krill	-0.9 ± 1.6	0.5 ± 3.0
	Control	-0.9 ± 2.3	0.7 ± 1.6
	Starved krill	1.8 ± 4.8	0.0 ± 1.7
	Control	-	-
	Carcass	10.0 ± 13.0 *	23.7 ± 26.8 *
	Control	-0.1 ± 0.1	0.0 ± 0.1

*Rates significantly different from 0.

both species, which coincided with relatively high rates of DON (and NH_4^+) release (Figures 3I, J) and relatively high respiration rates in the ambient seawater (Figures 3A, B). The overall average of DOC release rates was significantly higher for *M. norvegica* than for *T. raschii* carcasses (Mann-Whitney, U = 5, p = 0.011, n1 = n2 = 7).

DON release rates were approximately one order of magnitude lower than DOC release rates and showed similar trends of decreasing rates over time (Figures 3I, J). For *M. norvegica* carcasses, in particular, negative rates of DON release were reached from day 5 on, which indicates net uptake and/or consumption at the end of the incubation (Figure 3J). Ammonium release rates were similar to the DON release rates for *T. raschii* (Figure 3I; Mann-Whitney, U = 17, p = 0.383, n1 = n2 = 7) and significantly higher for *M. norvegica* carcasses (Figure 3J; Mann-Whitney, U = 0, p < 0.001, n1 = n2 = 7). Ammonium release was relatively constant over time, but for *M. norvegica* carcasses a particularly high release rate was observed on day 4 (Figure 3J). The overall average of NH_4^+ release rates was significantly higher for *M. norvegica* than for *T. raschii* carcasses (Mann-Whitney, U = 0, p < 0.001, n1 = n2 = 7).

Bacterial abundance in the seawater increased from ~10^6 to ~10^8 cells mL^{-1} at the end of the incubations with *T. raschii* carcasses, while in *M. norvegica* incubations, it ranged between ~10^6 and ~10^7 cells mL^{-1}. Assuming a BGE of 15% and a C:N ratio of 6.8 for a bacterial cell, 1.4 ± 0.4 and 5.0 ± 1.5 µmol C d^{-1}, and 0.2 ± 0.1 and 0.7 ± 0.2 µmol N d^{-1} were assimilated into total bacterial biomass (i.e., carcass-associated and free-living bacteria) in incubations with carcasses of *T. raschii* and *M. norvegica*, respectively, during the entire experimental period.

Carbon and nitrogen loss from sinking krill carcasses

After 7 days of degradation, non-significantly different percentages of 9.1% and 6.0% of the total organic carbon (Table 2) of *T. raschii* and *M. norvegica* carcasses, respectively, have been lost (Figures 5A, B; t-test, t = 1.606, df = 12, p = 0.134). During the first 4-5 days of degradation, loss of carbon from the carcasses occurred mainly in the form of DOC release, while afterward, total aerobic microbial respiration appeared as the main process utilizing the carbon from the carcasses. For the entire incubation period, however, the differences between cumulative DOC release and cumulative aerobic respiration were not statistically significant (Kruskal-Wallis, H = 29.815 (*T. raschii*), H = 29.761 (*M. norvegica*), df = 4, p < 0.001; Tukey *posthoc* p > 0.05). Carbon lost from the carcasses due to bacterial assimilation represented only a small percentage of the total carbon lost, accounting for <0.3% after 1 week of degradation. Anaerobic carbon mineralization through denitrification and DNRA was 2-4 orders of magnitude lower than through DOC release and aerobic respiration for both species (Supplementary Figure S4).

The cumulative loss of nitrogen from the carcasses after 7 days of degradation was 6.4% and 7.1% of the total nitrogen (Table 2) of *T. raschii* and *M. norvegica* carcasses, respectively, and these differences were not significantly different between krill species (Figures 5C, D; t-test, t = -0.283, df = 12, p = 0.782). During the first two days of incubation, loss of nitrogen in *T. raschii* carcasses occurred mainly through DON release, while after the third day, ammonium release appeared as the main contributor (Figure 5C). For the entire incubation period, however, the differences between cumulative DON and ammonium release from *T. raschii* carcasses were not statistically significant (Figure 6C; Mann-Whitney, U = 17, p = 0.383, n1 = n2 = 7). In *M. norvegica* carcasses, the most significant contribution to the loss of nitrogen from the carcasses was ammonium release (Figure 5D; Mann-Whitney, U = 0, p < 0.001, n1 = n2 = 7). Nitrogen used for bacterial assimilation accounted for 0.6% of the total nitrogen lost from the carcasses of the two species during the entire incubation period. This led to an overall C:N ratio of 7.2 and 6.2 for the

TABLE 2 Size, carbon, and nitrogen content, C:N molar ratio, sinking rates, and abundances of *Thysanoessa raschii* and *Meganyctiphanes norvegica*.

Krill species	Total length (mm)	Carbon (mg)	Nitrogen (mg)	C:N molar ratio	Carcass sinking rate (m d^{-1})	Abundance (ind m^{-2})*
T. raschii	24.2 ± 2.3 *n* = 24	14.1 ± 3.4 *n* = 5	3.5 ± 0.9 *n* = 5	4.8	1571 ± 163 *n* = 5	642
M. norvegica	41.8 ± 4.4 *n* = 22	75.3 *n* = 2	12.0 *n* = 2	7.3	3438 ± 470 *n* = 5	86.5

Mean ± standard deviation of n replicates is shown.
*Maximum values reported in Agersted and Nielsen, 2014.

organic matter lost from *T. raschii* and *M. norvegica* carcasses, respectively. This corresponds to 1.5 and 0.9-fold of the C:N ratios for fresh carcasses, respectively (Table 2).

Organic carbon fractions

T. raschii and *M. norvegica* carcasses were composed of organic carbon fractions of different reactivity. In fresh carcasses of both species, the organic carbon was 1-2% labile, 32-35% semi-labile, and 60-65% semi-refractory. The labile fraction decreased rapidly and was completely consumed during the first two days of degradation (Figure 6). Only ca. 6-10% of the semi-labile fraction was consumed during the entire incubation period in carcasses of both krill species. However, the slope of the regression line was not significantly different from 0 (t-test, t = -1.37, df = 4, p = 0.242 (*T. raschii*); t = -0.43, df = 1, p = 0.740 (*M. norvegica*)). The semi-refractory fractions thus remained statistically constant during the entire incubation period (t-test, t = -0.21, df = 4, p = 0.843 (*T. raschii*); t = 0.00, df = 1, p = 1.000 (*M. norvegica*)).

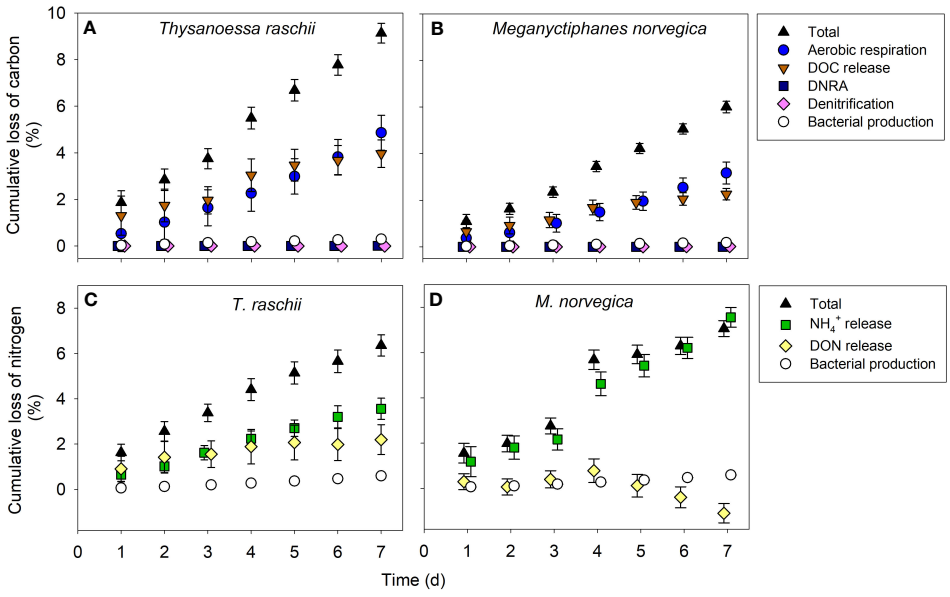

FIGURE 5
Cumulative loss of carbon and nitrogen from krill carcasses. Cumulative loss of carbon through aerobic respiration, Dissolved Organic Carbon (DOC) release, denitrification, dissimilatory nitrate reduction to ammonium (DNRA), and bacterial production in carcasses of **(A)** *Thysanoessa raschii* and **(B)** *Meganyctiphanes norvegica*. The contribution of denitrification and DNRA to carbon mineralization is presented in detail in the supplementary material (Supplementary Figure S4). Cumulative loss of nitrogen from krill carcasses through Dissolved Organic Nitrogen (DON) release, ammonium (NH_4^+) release, and bacterial production in carcasses of **(C)** *T. raschii* and **(D)** *M. norvegica*. Mean and standard deviations of 6-7 replicates are shown.

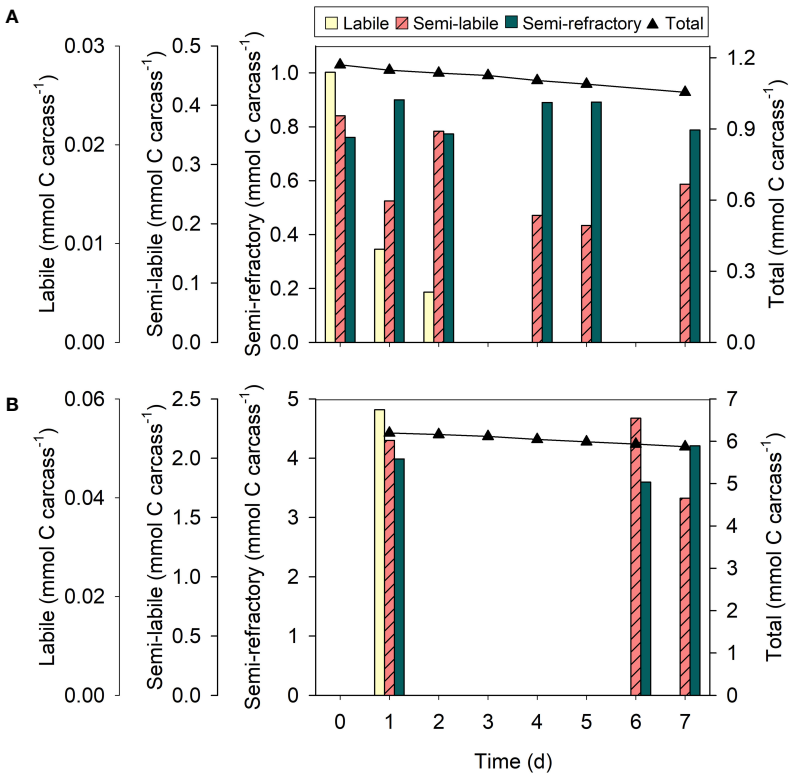

FIGURE 6
Organic carbon fractions of krill carcasses at different stages of degradation. Changes over time in organic carbon fractions associated with carcasses of **(A)** *Thysanoessa raschii* and **(B)** *Meganyctiphanes norvegica*. Black symbols represent the total amount of carbon in the carcasses per day. Only one carcass was measured per day.

Discussion

Degradation of krill carcasses in the Arctic

Our study revealed that the degradation of krill carcasses is mediated by the aerobic and anaerobic mineralization of particulate organic matter and the release of dissolved organic and inorganic compounds, sustaining ambient bacterial growth. After one week of simulated sinking through an oxygenated water column, <10% of the total carbon and <7% of the total nitrogen were lost from carcasses of *T. raschii* and *M. norvegica*. Carbon and nitrogen mineralization were mainly driven by aerobic microbial respiration. The assessment (using an RQ = 0.8) assumes that the oxygen consumption was due to aerobic microbial respiration and the reoxidation of NH_4^+ through nitrification (Paulmier et al., 2009). An unresolved fraction of total oxygen consumption may have also been due to the reoxidation of H_2S produced by sulfate reduction (Canfield et al., 1993) in the interior of the carcass; however, the carbon equivalents of the mineralization from sulfate reduction would be included in the derived O_2 consumption rates. An RQ of 0.8 is an average value that might differ from the organic material being degraded. However, using other realistic values for detrital material from literature (0.77-0.89; Alkemade et al., 1992; Hedges et al., 2002) would not significantly affect the derived budgets.

Anaerobic N-cycling taking place inside the carcasses also contributed to krill degradation as canonical (i.e., organoheterotrophic) denitrification and DNRA are fueled by the oxidation of organic matter. However, these processes occurred at rates two orders of magnitude lower than aerobic respiration rates, having a very limited quantitative significance for carbon mineralization during one week of carcass degradation. Despite their non-significant influence on particulate organic carbon mineralization, carcass-associated denitrification and DNRA proved important for pelagic N-cycling (see below).

Carcasses also released dissolved organic and inorganic compounds. DOC and DON were released at relatively high rates at the beginning of the incubations, probably associated with enzymatic hydrolysis (Urban-Rich, 1999) and leaching from the krill tissues (Lee and Fisher, 1992; Voss et al., 2013). NH_4^+ was released at relatively constant rates, and for *M. norvegica* it was the statistically more significant pathway of nitrogen loss from the carcasses. Ammonium was likely produced through the ammonification of organic matter by

heterotrophic bacteria (Gruber, 2008). Only ca. 1% of the NH_4^+ production occurring in the carcass incubations was due to DNRA activity. On the 4th day of degradation, an intermediate maximum of dissolved compound release from carcasses of both species coincided with the highest respiration rates in the seawater and a substantial increase in DNRA rates, at least for *T. raschii*. It can be speculated that the physical disintegration of the carcasses enhanced permeability and allowed the solute exchange with the surrounding water. DOC and DON leakage might have enabled higher respiration activity in the surrounding water, and nitrate intrusion probably sustained higher DNRA rates in the carcasses. Overall, ca. 50% of total aerobic microbial respiration occurred in the water surrounding the carcasses throughout the entire incubation period. In contrast, DNRA and denitrification rates were always negligible in the surrounding seawater and thus exclusively occurred within the O_2-depleted carcasses.

The C:N ratio of the carcasses of the two krill species remained approximately constant during the incubation period. This suggests that krill carcasses are still relatively N-rich when deposited at the seabed. The deposition of easy-to-degrade material associated with sinking krill carcasses will likely stimulate the consumption and recycling of organic substrates and inorganic nutrients by benthic heterotrophic communities (Albert et al., 2021). Indeed, the leakage of organic substrates and inorganic nutrients from the carcasses stimulated the growth and activity of bacteria in the surrounding seawater already during the sinking process. The abundance of free-living bacteria in the ambient seawater increased over time, and bacterial biomass production likely took place also directly associated with the carcasses. However, the calculated carbon and nitrogen utilization for biomass production in both carcass-associated and ambient bacteria was negligible for carbon and nitrogen loss from the carcasses, relative to the other processes quantified.

Anaerobic nitrogen cycling on sinking krill carcasses

Anaerobic N-cycling in the oxygen-depleted interior of carcasses was supported by oxygen micro-profile measurements. Generally, the microelectrode only reached the posterior part of the gut, but one micro-profile reached the midgut of a carcass of *M. norvegica* and confirmed persistent anoxia in the entire gut. Anoxia in the guts of live krill was detected irrespective of the feeding status of the animal. Surprisingly though, rates of anaerobic N-cycling were generally not significantly different from zero in live specimens of both species. This contrasts findings on diverse aquatic invertebrate species that, while alive, possess an anoxic gut and host high rates of denitrification and nitrous oxide production (Stief et al., 2009; Heisterkamp et al., 2010). The absence of the anaerobic N-cycling in starved animals can be expected because empty guts are probably more oxic and poorer in organic matter and microbial biomass than full guts (Stief et al., 2018). Nevertheless, limitations in the experimental design may have reduced the possibility to detect anaerobic processes in animals with full guts. In those incubations, only the seawater but not the food was ^{15}N-labeled. This, together with an effective filter-feeding system where the food particles are captured by krill while the water is expelled (Hamner et al., 1983; Tarling, 2010) may have decreased the incorporation of the labeled substrate into the digestive system of the animals and, consequently, the chance to track potential nitrogen transformations. More research and data about the microbial communities inhabiting krill guts will help to elucidate the apparent absence of the anaerobic N-cycling in live krill.

Since the final product of complete denitrification is N_2, this pathway results in the loss of fixed nitrogen (N-loss). To approximate the potential contribution of krill carcasses to pelagic N-loss, the standing stock of krill carcasses in the pelagic zone must be known. However, to date, the relative *in situ* abundance of carcasses in the Arctic has not been determined. Therefore, we made our estimations for two hypothetical scenarios: (a) low standing stock of carcasses based on krill mortality rates (i.e., 0.22% for *T. raschii* and 0.15% for *M. norvegica*) and (b) high standing stock of carcasses as could occur during a massive die-off (Fuentes et al., 2016) (i.e., 90% for both species). Based on the krill abundances in Table 2, scenario (a) results in an average of 1 and 0.2 carcasses m^{-2} of *T. raschii* and *M. norvegica*, respectively. Applying the carcass-specific denitrification rates of our incubations, pelagic denitrification rates would then amount to 0.01 and 0.02 μmol N m^{-2} d^{-1} for *T. raschii* and *M. norvegica* carcasses, respectively. In scenario (b), the carcass standing stock amounts to 575 and 78 carcasses m^{-2}, which translates into pelagic denitrification rates of 3.1 and 10 μmol N m^{-2} d^{-1} for *T. raschii* and *M. norvegica* carcasses, respectively. This means that despite their >7 times lower abundance, the larger *M. norvegica* carcasses contribute more to pelagic denitrification than *T. raschii* (Supplementary Table S1) due to significantly higher carcass-specific denitrification rates. The assessment hinges on the poorly defined abundance of krill carcasses, which can exhibit extensive spatio-temporal variations (Dalpapado and Skjoldal, 1991; Manno et al., 2020), and more data on krill carcass abundance in the Arctic are needed to better constrain these values. Anaerobic nitrogen cycling in other sinking particles with an anoxic interior, e.g., diatom aggregates (Stief et al., 2016) or cyanobacterial aggregates (Klawonn et al., 2015) has not been described for Arctic waters, but denitrification activity associated with sinking carcasses of the copepod *C. finmarchicus* in the same system corresponded to 0.06 μmol N m^{-2} d^{-1} (Glud et al., 2015), and denitrification associated with fecal pellets and carcasses of the larger copepod *C. hyperboreus* were estimated at up to 19.9 and 3.8 μmol N m^{-2} d^{-1}, respectively, in Disko Bay (West Greenland) (Stief et al., 2018). Reported rates of benthic denitrification in the coastal Arctic generally range between 15 and 900 μmol N m^{-2} d^{-1} (Supplementary Table S3). These

findings suggest that while microbial activity in zooplankton carcasses and fecal pellets represents a pelagic N-loss in Arctic waters, their contribution is minor relative to sedimentary denitrification (Supplementary Table S3), even in a scenario of massive krill death.

Sinking krill carcasses and the biological carbon pump

To assess the potential contribution of krill carcasses to the vertical carbon export in Nuup Kangerlua, their sinking flux must be approximated. To this end, we applied mortality rates of 0.15% d^{-1} (Lindley, 1980) and 0.22% d^{-1} (Tarling, 2010) and the maximum abundances in the fjord of 642 and 87 ind. m^{-2} (Table 2) for *T. raschii* and *M. norvegica*, respectively, which were all determined for the spring season. Assuming that most of the mortality is due to non-predatory causes, this would generate sinking fluxes of 1.0 carcasses m^{-2} d^{-1} for *T. raschii* and 0.2 carcasses m^{-2} d^{-1} for *M. norvegica*. Based on our measured sinking rates (Table 2), the carcasses will reach the deepest point of the fjord (625 m, Mortensen et al., 2011) in less than a day. During this short descent period, less than 2% of carcass-associated carbon would be lost, resulting in carbon deposition rates of 13.3 and 14.2 mg C m^{-2} d^{-1} for *T. raschii* and *M. norvegica*, respectively. These values are minor compared to the total POC flux in the fjord system (ca. 1500 mg C m^{-2} d^{-1}; Arendt et al., 2010).

However, a recent study in the Arctic Ocean reveals that the carbon demand by benthic communities exceeds by 3 to 46-fold the carbon flux out of the euphotic zone, suggesting the presence of unaccounted sources of POC to the vertical fluxes in the deep Arctic basins (Wiedmann et al., 2020). Our measurements show that the sinking flux of krill carcasses remains almost constant during descent due to low degradation rates and remarkably high sinking rates (i.e., 1500-3000 m d^{-1}). The sinking rates of krill carcasses measured in this study are up to 30 times higher than those of other particles like copepod carcasses and phytoplankton aggregates (Smetacek, 1985; Frangoulis et al., 2011) and relate well to sinking rates of krill fecal pellets (i.e., 30-1200 m d^{-1}; Cadée et al., 1992; Atkinson et al., 2012) and krill exuviae (i.e., 50-1000 m d^{-1}; Nicol and Stolp, 1989). Given those sinking velocities, krill carcasses may reach the bottom of the Arctic Ocean in 1-2 days. The apparent imbalance between pelagic supply and benthic requirement of organic carbon in the deep Arctic basins as derived by Wiedmann et al. (2020) is on average ~13.7 mg C m^{-2} d^{-1}. If this imbalance was to be closed by sinking krill carcasses, it would require a standing stock of approx. 600 ind. m^{-2} of *T. raschii* or 90 ind. m^{-2} of *M. norvegica*, which, assuming non-predatory mortality rates of 0.2% d^{-1}, would translate into export fluxes of 0.1 mg m^{-2} d^{-1} of labile carbon, 3-5 mg m^{-2} d^{-1} of semi-labile carbon, and 9-10 mg m^{-2} d^{-1} of semi-refractory carbon. This seems reasonable in specific areas of the Arctic Ocean where not only the targeted species, *T. raschii* and *M. norvegica*, inhabit but also *T. longicaudata* and *T. inermis* are found in high-density aggregations of 100->1000 ind. m^{-3} (Dalpadado and Skjoldal, 1996; Zhukova et al., 2009). *T. longicaudata* is herbivorous and has a similar carbon content to *T. raschii* (Agersted and Nielsen, 2014), while *T. inermis* is omnivorous and has a higher carbon content (Harvey et al., 2012; Agersted and Nielsen, 2014). We thus argue that the potential POC export per carcass of *T. longicaudata* and *T. inermis* will be similar to the *T. raschii* targeted in this study.

In the central Barents Sea, fecal pellets produced by krill have comprised a significant fraction (~40%) of the POC fluxes in summer (Riser et al., 2002). This dominance of krill fecal pellets must be sustained by considerable biomass of krill that has been reported to reach levels of ~1 g C m^{-2} in the area (Zhukova et al., 2009). Furthermore, the macromolecular composition of surface sediments across the Barents Sea exhibits high relative values of labile material related to chitin products (Stevenson and Abbott, 2019), suggesting that copepods or krill may be major contributors to benthic POC at the north of the Polar Front, at least transiently or in certain periods of the year (Zhukova et al., 2009; McQuinn et al., 2015).

Taken together, our results suggest that fast-sinking krill carcasses have the potential to export large amounts of semi-labile carbon from the epipelagic zone to the ocean interior in less than a day. This often-unaccounted source of carbon and nitrogen can fuel the benthic communities in the Arctic at fluxes as low as 1 carcass m^{-2} d^{-1} and thus, including krill carcasses in the budgets of the downward flux of POC may help to close the imbalance between sinking POC fluxes and benthic carbon demand in the area. However, caution needs to be taken when assessing the contribution of krill carcasses to the carbon budget in the Arctic. The patchy distribution of krill, and the inter-seasonal, inter-annual, and decadal variability of their populations (Zhukova et al., 2009; McQuinn et al., 2015, Edwards et al., 2021) will certainly restrict spatially and temporally the contribution of krill carcasses to the POC fluxes in the area. With more comprehensive data on the abundance and prevalence of krill carcasses throughout the year at hand, sinking krill carcasses will likely emerge as a relevant but episodic component of the biological carbon pump in the Arctic.

Data availability statement

The raw data supporting the conclusions of this article will be made available by the authors, without undue reservation.

Author contributions

RG, PS, BF-C, and TN contributed to the study's conception. BF-C, PS, AG, TN, and MW performed field and experimental work. BF-C, PS, LB, AG, AR, and HS performed sample and data

analyses. All authors contributed to data interpretation. BF-C, PS, and RG drafted the manuscript. The final submitted manuscript includes substantial input from all co-authors.

Funding

This work was funded by HADES-ERC Advanced Grant (No. 669947), the Danish National Research Foundation through the Danish Center for Hadal Research, HADAL (No. DNRF145) awarded to R.N. Glud, and the National Agency for Research and Development (ANID), Scholarship Program, Doctorado Becas Chile, 2017-72180314 awarded to BF-C.

Acknowledgments

The authors thank Rocío Rodríguez and Rodrigo Almeda for helping with krill collection and maintenance. The technical support by Else Ostermann, Birthe Christensen, Zarah Kofoed, and Lene Jakobsen is acknowledged.

Conflict of interest

The authors declare that the research was conducted in the absence of any commercial or financial relationships that could be construed as a potential conflict of interest.

Publisher's note

All claims expressed in this article are solely those of the authors and do not necessarily represent those of their affiliated organizations, or those of the publisher, the editors and the reviewers. Any product that may be evaluated in this article, or claim that may be made by its manufacturer, is not guaranteed or endorsed by the publisher.

Supplementary material

The Supplementary Material for this article can be found online at: https://www.frontiersin.org/articles/10.3389/fmars.2022.1019727/full#supplementary-material

References

Agersted, M. D., Bode, A., and Nielsen, T. G. (2014). Trophic position of coexisting krill species: a stable isotope approach. *Mar. Ecol. Prog. Ser.* 516, 139–151. doi: 10.3354/meps11055

Agersted, M. D., and Nielsen, T. G. (2014). Krill diversity and population structure along the sub-Arctic godthåbsfjord, SW Greenland. *J. Plankton Res.* 36, 800–815. doi: 10.1093/plankt/fbt139

Agersted, M. D., and Nielsen, T. G. (2016). Functional biology of sympatric krill species. *J. Plankton Res.* 38, 575–588. doi: 10.1093/plankt/fbw017

Albert, S., Bonaglia, S., Stjärnkvist, N., Winder, M., Thamdrup, B., and Nascimento, F. J. (2021). Influence of settling organic matter quantity and quality on benthic nitrogen cycling. *Limnol Oceanogr* 66, 1882–1895. doi: 10.1002/lno.11730

Alkemade, R., Wielemaker, A., De Jong, S., and Sandee, A. J. J. (1992). Experimental evidence for the role of bioturbation by the marine nematode *Diplolaimella dievengatensis* in stimulating the mineralization of *Spartina anglica* detritus. *Mar. Ecol. Prog. Ser.* 90, 149–155. doi: 10.3354/meps090149

Arendt, K. E., Nielsen, T. G., Rysgaard, S., and Tönnesson, K. (2010). Differences in plankton community structure along the godthåbsfjord, from the Greenland ice sheet to offshore waters. *Mar. Ecol. Prog. Ser.* 401, 49–62. doi: 10.3354/meps08368

Atkinson, A., Schmidt, K., Fielding, S., Kawaguchi, S., and Geissler, P. A. (2012). Variable food absorption by Antarctic krill: Relationships between diet, egestion rate and the composition and sinking rates of their fecal pellets. *Deep Sea Res Part II* 59, 147–158. doi: 10.1016/j.dsr2.2011.06.008

Belcher, A., Iversen, M., Manno, C., Henson, S. A., Tarling, G. A., and Sanders, R. (2016). The role of particle associated microbes in remineralization of fecal pellets in the upper mesopelagic of the Scotia Sea, Antarctica: Fecal pellet remineralization. *Limnol Oceanogr* 61, 1049–1064. doi: 10.1002/lno.10269

Berge, J., Cottier, F., Last, K. S., Varpe, Ø., Leu, E., Søreide, J., et al. (2009). Diel vertical migration of Arctic zooplankton during the polar night. *Biol. Lett.* 5, 69–72. doi: 10.1098/rsbl.2008.0484

Berline, L., Spitz, Y. H., Ashjian, C. J., Campbell, R. G., Maslowski, W., and Moore, S. E. (2008). Euphausiid transport in the western Arctic ocean. *Mar. Ecol. Prog. Ser.* 360, 163–178. doi: 10.3354/meps07387

Bourgeois, S., Archambault, P., and Witte, U. (2017). Organic matter remineralization in marine sediments: A pan-Arctic synthesis. *Global Biogeochem Cycles* 31, 190–213. doi: 10.1002/2016GB005378

Bower, C. E., and Holm-Hansen, T. (1980). A salicylate–hypochlorite method for determining ammonia in seawater. *Can. J. Fish Aquat Sci.* 37, 794–798. doi: 10.1139/f80-106

Cadée, G. C., González, H., and Schnack-Schiel, S. B. (1992). Krill diet affects faecal string settling. *Polar Biol.* 12, 75–80. doi: 10.1007/BF00239967

Canfield, D. E., Thamdrup, B., and Hansen, J. W. (1993). The anaerobic degradation of organic matter in Danish coastal sediments: Iron reduction, manganese reduction, and sulfate reduction. *Geochim Cosmochim Acta* 57, 3867–3883. doi: 10.1016/0016-7037(93)90340-3

Cavan, E. L., Belcher, A., Atkinson, A., Hill, S. L., Kawaguchi, S., McCormack, S., et al. (2019). The importance of Antarctic krill in biogeochemical cycles. *Nat. Commun.* 10, 4742. doi: 10.1038/s41467-019-12668-7

Chen, M., Huang, Y., Guo, L., Cai, P., Yang, W., Liu, G., et al. (2002). Biological productivity and carbon cycling in the Arctic ocean. *Chin. Sci. Bull.* 47, 1037–1040. doi: 10.1007/BF02907578

Dalpadado, P., and Skjoldal, H. R. (1996). Abundance, maturity and growth of the krill species *Thysanoessa inermis* and *T. longicaudata* in the barents Sea. *Mar. Ecol. Prog. Ser.* 144, 175–183. doi: 10.3354/meps144175

Dalsgaard, T., Thamdrup, B., Farías, L., and Revsbech, N. P. (2012). Anammox and denitrification in the oxygen minimum zone of the eastern south pacific. *Limnol Oceanogr* 57, 1331–1346. doi: 10.4319/lo.2012.57.5.1331

Del Giorgio, P. A., and Cole, J. J. (1998). Bacterial growth efficiency in natural aquatic systems. *Annu. Rev. Ecol. Syst.* 29, 503–541. doi: 10.1146/annurev.ecolsys.29.1.503

Ershova, E. A., and Kosobokova, K. N. (2019). Cross-shelf structure and distribution of mesozooplankton communities in the East-Siberian Sea and the adjacent Arctic ocean. *Polar Biol.* 42, 1353–1367. doi: 10.1007/s00300-019-02523-2

Falk-Petersen, S., Gatten, R. R., Sargent, J. R., and Hopkins, C. C. E. (1981). Ecological investigations on the zooplankton community in balsfjorden, northern Norway: seasonal changes in the lipid class composition of *Meganyctiphanes norvegica* (M. sars), *Thysanoessa raschii* (M. sars), and *T. inermis* (Krøyer). *J. Exp. Mar. Biol. Ecol.* 54, 209–224. doi: 10.1016/0022-0981(81)90158-1

Franco-Cisterna, B., Stief, P., and Glud, R. N. (2021). Temperature effects on carbon mineralization of sinking copepod carcasses. *Mar. Ecol. Prog. Ser.* 679, 31–45. doi: 10.3354/meps13907

Frangoulis, C., Skliris, N., Lepoint, G., Elkalay, K., Goffart, A., Pinnegar, J. K., et al. (2011). Importance of copepod carcasses versus faecal pellets in the upper water column of an oligotrophic area. *Estuarine Coast. Shelf Sci.* 92, 456–463. doi: 10.1016/j.ecss.2011.02.005

Fuentes, V., Alurralde, G., Meyer, B., Aguirre, G. E., Canepa, A., Wölfl, A. C., et al. (2016). Glacial melting: an overlooked threat to Antarctic krill. *Sci. Rep.* 6, 1–12. doi: 10.1038/srep27234

Fukuda, R., Ogawa, H., Nagata, T., and Koike, I. (1998). Direct determination of carbon and nitrogen contents of natural bacterial assemblages in marine environments. *Appl. Environ. Microbiol.* 64, 3352–3358. doi: 10.1128/AEM.64.9.3352-3358.1998

Gaillard, B., Meziane, T., Tremblay, R., Archambault, P., Blicher, M. E., Chauvaud, L., et al. (2017). Food resources of the bivalve astarte elliptica in a sub-Arctic fjord: a multi-biomarker approach. *Mar. Ecol. Prog. Ser.* 567, 139–156. doi: 10.3354/meps12036

Glud, R. N., Grossart, H. P., Larsen, M., Tang, K. W., Arendt, K. E., Rysgaard, S., et al. (2015). Copepod carcasses as microbial hot spots for pelagic denitrification. *Limnol Oceanogr* 60, 2026–2036. doi: 10.1002/lno.10149

Gómez-Gutiérrez, J., Peterson, W. T., De Robertis, A., and Brodeur, R. D. (2003). Mass mortality of krill caused by parasitoid ciliates. *Science* 301, 339–339. doi: 10.1126/science.1085164

Gruber, N. (2008). "The marine nitrogen cycle: Overview of distributions and processes," in *Nitrogen in the marine environment*. Eds. D. G. Capone, D. A. Bronk, M. R. Mulholland and E. J. Carpenter (Burlington, Amsterdam, San Diego, London: Elsevier), 1–50.

Halfter, S., Cavan, E. L., Butterworth, P., Swadling, K. M., and Boyd, P. W. (2022). "Sinking dead"–how zooplankton carcasses contribute to particulate organic carbon flux in the subantarctic southern ocean. *Limnol Oceanogr* 67, 13–25. doi: 10.1002/lno.11971

Hamner, W. M., Hamner, P. P., Strand, S. W., and Gilmer, R. W. (1983). Behavior of Antarctic krill, *Euphausia superba*: chemoreception, feeding, schooling, and molting. *Science* 220, 433–435. doi: 10.1126/science.220.4595.433

Harvey, H. R., Pleuthner, R. L., Lessard, E. J., Bernhardt, M. J., and Shaw, C. T. (2012). Physical and biochemical properties of the euphausiids *Thysanoessa inermis*, *Thysanoessa raschii*, and *Thysanoessa longipes* in the eastern Bering Sea. *Deep Sea Res Part II* 65, 173–183. doi: 10.1016/j.dsr2.2012.02.007

Hedges, J. I., Baldock, J. A., Gélinas, Y., Lee, C., Peterson, M. L., and Wakeham, S. G. (2002). The biochemical and elemental compositions of marine plankton: A NMR perspective. *Mar. Chem.* 78, 47–63. doi: 10.1016/S0304-4203(02)00009-9

Heisterkamp, I., Schramm, A., de Beer, D., and Stief, P. (2010). Nitrous oxide production associated with coastal marine invertebrates. *Mar. Ecol. Prog. Ser.* 415, 1–9. doi: 10.3354/meps08727

Iversen, M. H., and Ploug, H. (2013). Temperature effects on carbon-specific respiration rate and sinking velocity of diatom aggregates – potential implications for deep ocean export processes. *Biogeosciences* 10, 4073–4085. doi: 10.5194/bg-10-4073-2013

Kirchman, D. L., Morán, X. A. G., and Ducklow, H. (2009). Microbial growth in the polar oceans — role of temperature and potential impact of climate change. *Nat. Rev. Microbiol.* 7, 451–459. doi: 10.1038/nrmicro2115

Klawonn, I., Bonaglia, S., Brüchert, V., and Ploug, H. (2015). Aerobic and anaerobic nitrogen transformation processes in N_2-fixing cyanobacterial aggregates. *ISME J.* 9, 1456–1466. doi: 10.1038/ismej.2014.232

Lafargue, E., Marquis, F., and Pillot, D. (1998). Rock-eval 6 applications in hydrocarbon exploration, production, and soil contamination studies. *Rev. Inst. Fr. Pet* 53, 421–437. doi: 10.2516/ogst:1998036

Lee, B. ,. G., and Fisher, N. (1992). Decomposition and release of elements from zooplankton debris. *Mar. Ecol. Prog. Ser.* 88, 117–128. doi: 10.3354/meps088117

Lindley, J. A. (1980). Population dynamics and production of euphausiids II. *Thysanoessa inermis* and *T. raschii* in the north Sea and American coastal waters. *Mar. Biol.* 59, 225–233. doi: 10.1007/BF00404745

Manno, C., Fielding, S., Stowasser, G., Murphy, E. J., Thorpe, S. E., and Tarling, G. A. (2020). Continuous moulting by Antarctic krill drives major pulses of carbon export in the north Scotia Sea, southern ocean. *Nat. Commun.* 11, 6051. doi: 10.1038/s41467-020-19956-7

Mauchline, J., and Fisher, J. R. (1969). The biology of euphausiids. *Adv. Mar. Biol.* 7, 1–454. doi: 10.1016/S0065-2881(08)60468-X

McBride, M. M., Dalpadado, P., Drinkwater, K. F., Godø, O. R., Hobday, A. J., Hollowed,, et al. (2014). Krill, climate, and contrasting future scenarios for Arctic and Antarctic fisheries. *ICES J. Mar. Sci.* 71, 1934–1955. doi: 10.1093/icesjms/fsu002

McQuinn, I. H., Plourde, S., St. Pierre, J. F., and Dion, M. (2015). Spatial and temporal variations in the abundance, distribution, and aggregation of krill (*Thysanoessa raschii* and *Meganyctiphanes norvegica*) in the lower estuary and gulf of st. Lawrence. *Prog. Oceanogr* 131, 159–176. doi: 10.1016/j.pocean.2014.12.014

Mortensen, J., Lennert, K., Bendtsen, J., and Rysgaard, S. (2011). Heat sources for glacial melt in a sub-Arctic fjord (Godthåbsfjord) in contact with the Greenland ice sheet. *J. Geophys. Res.* 116, C01013. doi: 10.1029/2010JC006528

Nelson, C. E., and Wear, E. K. (2014). Microbial diversity and the lability of dissolved organic carbon. *Proc. Natl. Acad. Sci. U.S.A.* 111, 7166–7167. doi: 10.1073/pnas.1405751111

Nicol, S., and Stolp, M. (1989). Sinking rates of cast exoskeletons of Antarctic krill (*Euphausia superba* Dana) and their role in the vertical flux of particulate matter and fluoride in the southern ocean. *Deep Sea Res Part I* 36, 1753–1762. doi: 10.1016/0198-0149(89)90070-8

Ostapenia, A. P., Parparov, A., and Berman, T. (2009). Lability of organic carbon in lakes of different trophic status. *Freshw. Biol.* 54, 1312–1323. doi: 10.1111/j.1365-2427.2009.02183.x

Pauli, N. C., Flintrop, C. M., Konrad, C., Pakhomov, E. A., Swoboda, S., Koch, F., et al. (2021). Krill and salp faecal pellets contribute equally to the carbon flux at the Antarctic peninsula. *Nat. Commun.* 12, 1–12. doi: 10.1038/s41467-021-27436-9

Paulmier, A., Kriest, I., and Oschlies, A. (2009). Stoichiometries of remineralisation and denitrification in global biogeochemical ocean models. *Biogeosciences* 6, 923–935. doi: 10.5194/bg-6-923-2009

Revsbech, N. P. (1989). An oxygen microsensor with a guard cathode. *Limnol Oceanogr* 34, 474–478. doi: 10.4319/lo.1989.34.2.0474

Riser, C., Wassmann, P., Olli, K., Pasternak, A., and Arashkevich, E. (2002). Seasonal variation in production, retention and export of zooplankton faecal pellets in the marginal ice zone and central barents Sea. *J. Mar. Syst.* 38, 175–188. doi: 10.1016/S0924-7963(02)00176-8

Rudra, A., Sanei, H., Nytoft, H. P., Petersen, H. I., Blok, C., Bodin, S., et al. (2021). Organic matter characterization of the lower Cretaceous tight reservoirs in the Danish north Sea. *Int. J. Coal Geol.* 238, 103714. doi: 10.1016/j.coal.2021.103714

Sanei, H., Wood, J. M., Ardakani, O. H., Clarkson, C. R., and Jiang, C. (2015). Characterization of organic matter fractions in an unconventional tight gas siltstone reservoir. *Int. J. Coal Geol.* 150–151, 296–305. doi: 10.1016/j.coal.2015.04.004

Silva, T., Gislason, A., Astthorsson, O. S., and Marteinsdóttir, G. (2017). Distribution, maturity and population structure of *Meganyctiphanes norvegica* and *Thysanoessa inermis* around Iceland in spring. *PloS One* 12, e0187360. doi: 10.1371/journal.pone.0187360

Smetacek, V. S. (1985). Role of sinking in diatom life-history cycles: ecological, evolutionary and geological significance. *Mar. Biol.* 84, 239–251. doi: 10.1007/BF00392493

Sokolova, M. N. (1994). Euphausiid "dead body rain" as a source of food for abyssal benthos. *Deep Sea Res. Part I*, 41(4), 741–746. doi: 10.1016/0967-0637(94)90052-3

Stevenson, M. A., and Abbott, G. D. (2019). Exploring the composition of macromolecular organic matter in Arctic ocean sediments under a changing sea ice gradient. *J. Anal. Appl. Pyrolysis* 140, 102–111. doi: 10.1016/j.jaap.2019.02.006

Stief, P., Kamp, A., Thamdrup, B., and Glud, R. N. (2016). Anaerobic nitrogen turnover by sinking diatom aggregates at varying ambient oxygen levels. *Front. Microbiol.* 7. doi: 10.3389/fmicb.2016.00098

Stief, P., Lundgaard, A. S. B., Morales-Ramírez, Á., Thamdrup, B., and Glud, R. N. (2017). Fixed-nitrogen loss associated with sinking zooplankton carcasses in a coastal oxygen minimum zone (Golfo dulce, Costa Rica). *Front. Mar. Sci.* 4. doi: 10.3389/fmars.2017.00152

Stief, P., Lundgaard, A., Nielsen, T. G., and Glud, R. N. (2018). Feeding-related controls on microbial nitrogen cycling associated with the Arctic marine copepod *Calanus hyperboreus*. *Mar. Ecol. Prog. Ser.* 602, 1–14. doi: 10.3354/meps12700

Stief, P., Poulsen, M., Nielsen, L. P., Brix, H., and Schramm, A. (2009). Nitrous oxide emission by aquatic macrofauna. *Proc. Natl. Acad. Sci. U.S.A.* 106, 4296–4300. doi: 10.1073/pnas.0808228106

Tang, K. W., Backhaus, L., Riemann, L., Koski, M., Grossart, H. P., Munk, P., et al. (2019). Copepod carcasses in the subtropical convergence zone of the Sargasso Sea: implications for microbial community composition, system respiration and carbon flux. *J. Plankton Res.* 41, 549–560. doi: 10.1093/plankt/fbz038

Tang, K. W., and Elliott, D. T. (2014). "Copepod carcasses: occurrence, fate and ecological importance," in *Copepods: diversity, habitat and behavior*. Ed. L. Seuront (New York: Nova Science Publishers), 255–278.

Tang, K. W., Glud, R. N., Glud, A., Rysgaard, S., and Nielsen, T. G. (2011). Copepod guts as biogeochemical hotspots in the sea: Evidence from microelectrode profiling of *Calanus* spp. *Limnol Oceanogr* 56, 666–672. doi: 10.4319/lo.2011.56.2.0666

Tarling, G. A. (2010). Population dynamics of northern krill (*Meganyctiphanes norvegica* sars). *Adv. Mar. Biol.* 57, 59–90. doi: 10.1016/B978-0-12-381308-4.00003-0

Thamdrup, B. (2012). New pathways and processes in the global nitrogen cycle. *Annu. Rev. Ecol. Evol. Syst.* 43, 407–428. doi: 10.1146/annurev-ecolsys-102710-145048

Urban-Rich, J. (1999). Release of dissolved organic carbon from copepod fecal pellets in the Greenland Sea. *J. Exp. Mar. Biol. Ecol.* 232, 107–124. doi: 10.1016/S0022-0981(98)00104-X

Voss, M., Bange, H. W., Dippner, J. W., Middelburg, J. J., Montoya, J. P., and Ward, B. (2013). The marine nitrogen cycle: recent discoveries, uncertainties and the potential relevance of climate change. *Phil Trans. R. Soc B.* 368, 20130121. doi: 10.1098/rstb.2013.0121

Warembourg, F. R. (1993). "Nitrogen fixation in soil and plant systems," in *Nitrogen isotope techniques*. Eds. R. Knowles and T. H. Blackburn (San Diego: Academic), 127–156.

Werner, I. (2000). Faecal pellet production by Arctic under-ice amphipods–transfer of organic matter through the ice/water interface. *Hydrobiologia* 426, 89–96. doi: 10.1023/A:1003984327103

Wheeler, P. A., Gosselin, M., Sherr, E., Thibaultc, D., Kirchman, D. L., Benner, R., et al. (1996). Active cycling of organic carbon in the central Arctic ocean. *Nature* 380, 697–699. doi: 10.1038/380697a0

Wiedmann, I., Ershova, E., Bluhm, B. A., Nöthig, E. M., Gradinger, R. R., Kosobokova, K., et al. (2020). What feeds the benthos in the Arctic basins? assembling a carbon budget for the deep Arctic ocean. *Front. Mar. Sci.* 7. doi: 10.3389/fmars.2020.00224

Zhukova, N. G., Nesterova, V. N., Prokopchuk, I. P., and Rudneva, G. B. (2009). Winter distribution of euphausiids (Euphausiacea) in the barents Sea, (2000–2005). *Deep Sea Res. Part II* 56, 1959–1967. doi: 10.1016/j.dsr2.2008.11.007